Journal of Computational and Applied Mathematics 285 (2015) 45–58

Contents lists available at ScienceDirect

Journal of Computational and Applied Mathematics

journal homepage: www.elsevier.com/locate/cam

A weak Galerkin finite element method with polynomial reduction

Lin Mu [a], Junping Wang [b], Xiu Ye [c,*]

[a] Department of Mathematics, Michigan State University, East Lansing, MI 48824, United States
[b] Division of Mathematical Sciences, National Science Foundation, Arlington, VA 22230, United States
[c] Department of Mathematics, University of Arkansas at Little Rock, Little Rock, AR 72204, United States

ARTICLE INFO

Article history:
Received 28 July 2014
Received in revised form 27 October 2014

MSC:
primary 65N15
65N30
secondary 35J50

Keywords:
Weak Galerkin
Finite element methods
Weak gradient
Discrete weak gradient
Second-order elliptic equation
Polyhedral meshes

ABSTRACT

The weak Galerkin (WG) is a novel numerical method based on variational principles for weak functions and their weak partial derivatives defined as distributions. In the implementation, the weak partial derivatives and the weak functions are approximated by polynomials with various degrees of freedom. The accuracy and the computational complexity of the corresponding WG scheme is significantly impacted by the selection of such polynomials. This paper presents an optimal combination for the polynomial spaces that minimize the number of unknowns in the numerical scheme without compromising the accuracy of the numerical approximation. For illustrative purpose, the authors use the second order elliptic equation to demonstrate the basic ideas of polynomial reduction. Consequently, a new weak Galerkin finite element method is proposed and analyzed. Error estimates of optimal order are established for the corresponding WG approximations in both a discrete H^1 norm and the standard L^2 norm. In addition, the paper presents some numerical results to demonstrate the power of the WG method in dealing with finite element partitions with arbitrary polygons in 2D or polyhedra in 3D. The numerical examples include various finite element partitions such as triangular mesh, quadrilateral mesh, honeycomb mesh in 2D and mesh with deformed cubes in 3D.

1. Introduction

This paper is concerned with new development of weak Galerkin (WG) finite element methods by presenting and analyzing an optimal combination of polynomials in the design of finite element spaces. In general, WG refers to a finite element technique for partial differential equations in which differential operators (e.g., gradient, divergence, curl, Laplacian) are interpreted and approximated as linear functionals in the space of weak functions. For second order elliptic equations, the weak functions possess the form of $v = \{v_0, v_b\}$ with $v = v_0$ representing the value of v in the interior of each element and $v = v_b$ on the boundary of the element. Both v_0 and v_b are approximated by polynomials of various degrees in the numerical approximation. More precisely, denote by $P_\ell(T) \times P_s(e)$ the approximating polynomial spaces for $\{v_0, v_b\}$, where e stands for the edge or face of T, ℓ and s are non-negative integers. The weak partial derivatives are defined for weak functions in the sense of distributions by including the boundary information. In the WG finite element method, the weak partial derivatives are approximated by polynomials of degree m; i.e., $P_m(T)$. Thus, each combination of $(P_\ell(T), P_s(e), [P_m(T)]^d)$

* Corresponding author.
E-mail addresses: linmu@math.msu.edu (L. Mu), jwang@nsf.gov (J. Wang), xxye@ualr.edu (X. Ye).

http://dx.doi.org/10.1016/j.cam.2015.02.001
0377-0427/

leads to a weak Galerkin finite element method for the PDEs under consideration. For a prescribed accuracy of h^k, we ask the following question: For what combination of (ℓ, s, m), the corresponding WG scheme shall involve the least number of unknowns in implementation. This shall be referred to as polynomial optimality problem.

For simplicity, we demonstrate the polynomial optimality by using the second order elliptic equation with Dirichlet boundary condition. The model problem seeks an unknown function u satisfying

$$-\nabla\cdot(a\nabla u) = f, \quad \text{in } \Omega, \tag{1.1}$$

$$u = g, \quad \text{on } \partial\Omega, \tag{1.2}$$

where Ω is a polytopal domain in $\mathbb{R}^d$ (polygonal or polyhedral domain for $d = 2, 3$), ∇u denotes the gradient of the function u, and a is a symmetric $d \times d$ matrix-valued function in Ω. Assume that there exist two positive numbers $\lambda_1, \lambda_2 > 0$ such that

$$\lambda_1\xi^t\xi \le \xi^t a\xi \le \lambda_2\xi^t\xi, \quad \forall\xi \in \mathbb{R}^d. \tag{1.3}$$

Here ξ is understood as a column vector and ξ^t is the transpose of ξ.

A weak Galerkin finite element method was introduced and analyzed in [1] for the model problem (1.1)–(1.2) in the primal formulation, in which the polynomial configuration was given by either $(P_{k-1}(T), P_{k-1}(e), RT_{k-1}(T))$ or $(P_{k-1}(T), P_k(e), [P_k(T)]^d)$. Here $RT_j(T)$ is the Raviart–Thomas space of order $j \ge 0$. In other words, the discrete weak gradient is computed by using polynomials of degree higher than that of v_0. However, the WG finite element schemes in [1] are limited to the classical finite element partitions consisting of triangles ($d = 2$) or tetrahedra ($d = 3$). Following the stabilization approach of [2] for the mixed formulation, we developed a new class of WG finite element method in [3] for the primal formulation by allowing the use of finite elements of arbitrary shape. In particular, the WG finite element scheme in [3] is based on the polynomial combination of $(P_k(T), P_k(e), [P_{k-1}(T)]^d)$ so that the discrete weak gradient is computed in a polynomial space with degree lower than that of v_0. But the use of $(P_k(T), P_k(e))$ for $\{v_0, v_b\}$ indicates that the WG scheme in [3] involves more unknowns than that of [1] for the given accuracy of h^k in the H^1 norm.

The first objective of this paper is to present and analyze a new combination of polynomial spaces that reduces the number of unknowns of [3] without compromising the order of accuracy for the corresponding WG finite element scheme. Specifically, this new WG finite element scheme uses $(P_k(T), P_{k-1}(e), [P_{k-1}(T)]^d)$, and the corresponding WG solution converges to the exact solution of (1.1)–(1.2) with the optimal order of $O(h^k)$ in H^1 and $O(h^{k+1})$ in L^2. We emphasize that the unknowns associated with v_0 can be eliminated locally on each element in terms of the unknowns for v_b. Therefore, for problems in 2D, the global stiffness matrix can be formulated by involving only the unknowns of v_b on the set of edges of the finite element partition. In this sense, the new WG formulation of $(P_k(T), P_{k-1}(e), [P_{k-1}(T)]^d)$ reduces the size of unknowns by half from the formulation of $(P_k(T), P_k(e), [P_{k-1}(T)]^d)$ for the lowest order element (i.e., $k = 1$). It can be seen from Theorems 6.2 and 6.4 that the WG formulation of $(P_1(T), P_0(e), [P_0(T)]^d)$ converges with the rate of $O(h)$ in H^1 and $O(h^2)$ in L^2 norm. We believe that the formulation of $(P_1(T), P_0(e), [P_0(T)]^d)$ minimizes the number of unknowns for all the WG finite element methods of $(P_\ell(T), P_s(e), [P_m(T)]^d)$ with the rate of $O(h)$ in H^1 and $O(h^2)$ in L^2 norm. More comparisons will be conducted in future research.

The second objective of this paper is to study the reliability, flexibility and accuracy of the weak Galerkin method through numerical experiments. To this end, the first and second order weak Galerkin elements are implemented on partitions with different shape of polygons and polyhedra. Our numerical results show optimal order of convergence for $k = 1, 2$ on triangular, quadrilateral, and honeycomb meshes in 2D and deformed cubes in 3D. The numerical results are in great consistency with the convergence theory.

It has been proved rigorously in [2] that polynomials of P_k type can be used in weak Galerkin finite element methods on any polygonal/polyhedral elements. This contrasts to the use of polynomials P_k for triangular elements and tensor products Q_k for rectangular elements in the classical finite element methods. In practice, allowing arbitrary shape in finite element partition provides a great flexibility in both numerical approximation and mesh generation, especially in regions where the domain geometry is complex. The results of the present paper indicate that the same flexibility is enjoyed by the WG finite element method in the primal formulation.

One close relative of the WG finite element method of this paper is the hybridizable discontinuous Galerkin (HDG) method [4]. For the second order elliptic problem (1.1)–(1.2) in primal formulation, these two methods share the same feature of approximating the first order derivatives or fluxes through a formula that was commonly employed in the mixed finite element method. Note that the two methods are different for problems with variable coefficients. For high order PDEs, such as the biharmonic equation [5,6], the WG method is greatly different from the HDG. It should be emphasized that the concept of weak derivatives makes WG a widely applicable numerical technique for a large variety of partial differential equations which we shall report in forthcoming papers.

The paper is organized as follows. In Section 2, we shall review the definition of the weak gradient operator and its discrete analogue. In Section 3, we shall describe a new WG scheme. Section 4 will be devoted to a discussion of mass conservation for the WG scheme. In Section 5, we shall present some technical estimates for the usual L^2 projection operators. Section 6 is used to derive an optimal order error estimate for the WG approximation in both H^1 and L^2 norms. Finally in Section 7, we shall present some numerical results that confirm the theory developed in earlier sections.

2. Weak gradient and discrete weak gradient

Let T be any polytopal domain with boundary ∂T. A *weak function* on the region T refers to a function $v = \{v_0, v_b\}$ such that $v_0 \in L^2(T)$ and $v_b \in L^2(\partial T)$. The first component v_0 can be understood as the value of v in T, and the second component v_b represents v on the boundary of T. Note that v_b may not necessarily be related to the trace of v_0 on ∂T should a trace be well-defined. Denote by $W(T)$ the space of weak functions on T; i.e.,

$$W(T) = \{v = \{v_0, v_b\} : \ v_0 \in L^2(T), \ v_b \in L^2(\partial T)\}. \tag{2.1}$$

Define $(v, w)_D = \int_D vw dx$ with $D \subset \mathbb{R}^d$ and $\langle v, w\rangle_\gamma = \int_\gamma vw ds$ with $\gamma \subset \mathbb{R}^{d-1}$.

Definition 2.1. For any $v \in W(T)$, the *weak gradient* of v is defined as a linear functional $\nabla_w v$ in the dual space of $H^1(T)$ whose action on each $q \in [H^1(T)]^d$ is given by

$$\langle \nabla_w v, q\rangle_T = -(v_0, \nabla \cdot q)_T + \langle v_b, q \cdot \mathbf{n}\rangle_{\partial T}, \tag{2.2}$$

where $\mathbf{n}$ is the outward normal direction to ∂T, $(v_0, \nabla \cdot q)_T = \int_T v_0(\nabla \cdot q)dT$ is the inner product of v_0 and $\nabla \cdot q$ in $L^2(K)$, and $\langle v_b, q \cdot \mathbf{n}\rangle_{\partial T}$ is the inner product of v_b and $q \cdot \mathbf{n}$ in $L^2(\partial T)$.

The Sobolev space $H^1(T)$ can be embedded into the space $W(T)$ by an inclusion map $i_W : \ H^1(T) \to W(T)$ defined as follows

$$i_W(\phi) = \{\phi|_T, \phi|_{\partial T}\}, \quad \phi \in H^1(T).$$

With the help of the inclusion map i_W, the Sobolev space $H^1(T)$ can be viewed as a subspace of $W(T)$ by identifying each $\phi \in H^1(T)$ with $i_W(\phi)$. Analogously, a weak function $v = \{v_0, v_b\} \in W(T)$ is said to be in $H^1(T)$ if it can be identified with a function $\phi \in H^1(T)$ through the above inclusion map. It is not hard to see that the weak gradient is identical with the strong gradient (i.e., $\nabla_w v = \nabla v$) for smooth functions $v \in H^1(T)$.

Denote by $P_r(T)$ the set of polynomials on T with degree no more than r. We can define a discrete weak gradient operator by approximating ∇_w in a polynomial subspace of the dual of $[H^1(T)]^d$.

Definition 2.2. The discrete weak gradient operator, denoted by $\nabla_{w,r,T}$, is defined as the unique polynomial $(\nabla_{w,r,T} v) \in [P_r(T)]^d$ satisfying the following equation

$$(\nabla_{w,r,T} v, q)_T = -(v_0, \nabla \cdot q)_T + \langle v_b, q \cdot \mathbf{n}\rangle_{\partial T}, \quad \forall q \in [P_r(T)]^d. \tag{2.3}$$

By applying the usual integration by parts to the first term on the right hand side of (2.3), we can rewrite Eq. (2.3) as follows

$$(\nabla_{w,r,T} v, q)_T = (\nabla v_0, q)_T + \langle v_b - v_0, q \cdot \mathbf{n}\rangle_{\partial T}, \quad \forall q \in [P_r(T)]^d. \tag{2.4}$$

3. Weak Galerkin finite element schemes

Let $\mathcal{T}_h$ be a partition of the domain Ω consisting of polygons in two dimension or polyhedra in three dimension satisfying a set of conditions specified in [2]. Denote by $\mathcal{E}_h$ the set of all edges or flat faces in $\mathcal{T}_h$, and let $\mathcal{E}_h^0 = \mathcal{E}_h \setminus \partial\Omega$ be the set of all interior edges or flat faces. For every element $T \in \mathcal{T}_h$, we denote by h_T its diameter and mesh size $h = \max_{T\in\mathcal{T}_h} h_T$ for $\mathcal{T}_h$. Assume that the mesh is quasi-uniform in the sense that there exists a constant C such that $h \le Ch_T$ for all $T \in \mathcal{T}_h$.

For a given integer $k \ge 1$, let V_h be the weak Galerkin finite element space associated with $\mathcal{T}_h$ defined as follows

$$V_h = \{v = \{v_0, v_b\} : \ v_0|_T \in P_k(T), \ v_b|_e \in P_{k-1}(e), \ e \subset \partial T, T \in \mathcal{T}_h\} \tag{3.1}$$

and

$$V_h^0 = \{v : \ v \in V_h, \ v_b = 0 \text{ on } \partial\Omega\}. \tag{3.2}$$

We would like to emphasize that any function $v \in V_h$ has a single value v_b on each edge $e \in \mathcal{E}_h$.

For each element $T \in \mathcal{T}_h$, denote by Q_0 the L^2 projection from $L^2(T)$ to $P_k(T)$ and by Q_b the L^2 projection from $L^2(e)$ to $P_{k-1}(e)$. Denote by $\mathbb{Q}_h$ the L^2 projection from $[L^2(T)]^d$ to the local discrete gradient space $[P_{k-1}(T)]^d$. Let $V = H^1(\Omega)$. We define a projection operator $Q_h : V \to V_h$ so that on each element $T \in \mathcal{T}_h$

$$Q_h v = \{Q_0 v_0, Q_b v_b\}, \qquad \{v_0, v_b\} = i_W(v) \in W(T). \tag{3.3}$$

Denote by $\nabla_{w,k-1}$ the discrete weak gradient operator on the finite element space V_h computed by using (2.3) on each element T; i.e.,

$$(\nabla_{w,k-1} v)|_T = \nabla_{w,k-1,T}(v|_T), \quad \forall v \in V_h.$$

For simplicity, from now on we shall drop the subscript $k-1$ from the notation $\nabla_{w,k-1}$ for the discrete weak gradient.

Now we introduce two forms on V_h as follows:

$$a(v, w) = \sum_{T\in\mathcal{T}_h} (a\nabla_w v, \nabla_w w)_T,$$

$$s(v, w) = \rho \sum_{T\in\mathcal{T}_h} h_T^{-1} \langle Q_b v_0 - v_b, Q_b w_0 - w_b\rangle_{\partial T},$$

where ρ is any positive number. For simplicity, we shall take $\rho = 1$ throughout the paper. Denote by $a_s(\cdot, \cdot)$ a stabilization of $a(\cdot, \cdot)$ given by

$$a_s(v, w) = a(v, w) + s(v, w).$$

Weak Galerkin Algorithm 1. Find $u_h = \{u_0, u_b\} \in V_h$ such that $u_b = Q_b g$ on $\partial\Omega$ and satisfying the following equations:

$$a_s(u_h, v) = (f, v_0), \quad \forall\, v = \{v_0, v_b\} \in V_h^0. \tag{3.4}$$

Next, we justify the well-posedness of the scheme (3.4). For any $v \in V_h$, let

$$|||v||| := \sqrt{a_s(v, v)}. \tag{3.5}$$

The functional $|||\cdot|||$ defines a semi-norm in V_h. It also defines a norm in V_h^0. To verify this, it suffices to check the positivity property for $|||\cdot|||$. To this end, assume that $v \in V_h^0$ and $|||v||| = 0$. It follows that

$$(a\nabla_w v, \nabla_w v) + \sum_{T\in\mathcal{T}_h} h_T^{-1} \langle Q_b v_0 - v_b, Q_b v_0 - v_b\rangle_{\partial T} = 0,$$

which implies that $\nabla_w v = 0$ on each element T and $Q_b v_0 = v_b$ on ∂T. It follows from $\nabla_w v = 0$ and (2.4) that for any $q \in [P_{k-1}(T)]^d$

$$\begin{aligned} 0 &= (\nabla_w v, q)_T \\ &= (\nabla v_0, q)_T - \langle v_0 - v_b, q\cdot\mathbf{n}\rangle_{\partial T} \\ &= (\nabla v_0, q)_T - \langle Q_b v_0 - v_b, q\cdot\mathbf{n}\rangle_{\partial T} \\ &= (\nabla v_0, q)_T. \end{aligned}$$

Letting $q = \nabla v_0$ in the equation above yields $\nabla v_0 = 0$ on $T \in \mathcal{T}_h$. Thus, $v_0 = const$ on every $T \in \mathcal{T}_h$. This, together with the fact that $Q_b v_0 = v_b$ on ∂T and $v_b = 0$ on $\partial\Omega$, implies that $v_0 = v_b = 0$.

Lemma 3.1. *The weak Galerkin finite element scheme (3.4) has one and only one solution.*

Proof. It suffices to prove the uniqueness. If $u_h^{(1)}$ and $u_h^{(2)}$ are two solutions of (3.4), then $e_h = u_h^{(1)} - u_h^{(2)}$ would satisfy the following equation

$$a_s(e_h, v) = 0, \quad \forall v \in V_h^0.$$

Note that $e_h \in V_h^0$. Then by letting $v = e_h$ in the above equation we arrive at

$$|||e_h|||^2 = a_s(e_h, e_h) = 0.$$

It follows that $e_h \equiv 0$, or equivalently, $u_h^{(1)} \equiv u_h^{(2)}$. This completes the proof of the lemma. □

4. Mass conservation

The second order elliptic equation (1.1) can be rewritten in a conservative form as follows:

$$\nabla\cdot q = f, \quad q = -a\nabla u.$$

Let T be any control volume. Integrating the first equation over T yields the following integral form of mass conservation:

$$\int_{\partial T} q\cdot\mathbf{n} ds = \int_T f dT. \tag{4.1}$$

We claim that the numerical approximation from the weak Galerkin finite element method (3.4) for (1.1) retains the mass conservation property (4.1) with an appropriately defined numerical flux q_h. To this end, for any given $T \in \mathcal{T}_h$, we chose in (3.4) a test function $v = \{v_0, v_b = 0\}$ so that $v_0 = 1$ on T and $v_0 = 0$ elsewhere. It follows from (3.4) that

$$\int_T a\nabla_w u_h \cdot \nabla_w v dT + h_T^{-1} \int_{\partial T} (Q_b u_0 - u_b) ds = \int_T f dT. \tag{4.2}$$

Using the definition (2.3) for $\nabla_w v$ one arrives at

$$\begin{aligned}\int_T a\nabla_w u_h \cdot \nabla_w v dT &= \int_T \mathbb{Q}_h(a\nabla_w u_h)\cdot \nabla_w v dT \\ &= -\int_T \nabla\cdot \mathbb{Q}_h(a\nabla_w u_h) dT \\ &= -\int_{\partial T} \mathbb{Q}_h(a\nabla_w u_h)\cdot \mathbf{n} ds. \end{aligned} \tag{4.3}$$

Substituting (4.3) into (4.2) yields

$$\int_{\partial T} \left\{-\mathbb{Q}_h\left(a\nabla_w u_h\right) + h_T^{-1}(Q_b u_0 - u_b)\mathbf{n}\right\}\cdot \mathbf{n} ds = \int_T f dT, \tag{4.4}$$

which indicates that the weak Galerkin method conserves mass with a numerical flux given by

$$q_h = -\mathbb{Q}_h\left(a\nabla_w u_h\right) + h_T^{-1}(Q_b u_0 - u_b)\mathbf{n}.$$

Next, we verify that the normal component of the numerical flux, namely $q_h\cdot\mathbf{n}$, is continuous across the edge of each element T. To this end, let e be an interior edge/face shared by two elements T_1 and T_2. Choose a test function $v = \{v_0, v_b\}$ so that $v_0 \equiv 0$ and $v_b = 0$ everywhere except on e. It follows from (3.4) that

$$\int_{T_1\cup T_2} a\nabla_w u_h\cdot\nabla_w v dT - h_{T_1}^{-1}\int_{\partial T_1\cap e}(Q_b u_0 - u_b)|_{T_1} v_b ds - h_{T_2}^{-1}\int_{\partial T_2\cap e}(Q_b u_0 - u_b)|_{T_2} v_b ds = 0. \tag{4.5}$$

Using the definition of weak gradient (2.3) we obtain

$$\begin{aligned}\int_{T_1\cup T_2} a\nabla_w u_h\cdot\nabla_w v dT &= \int_{T_1\cup T_2}\mathbb{Q}_h(a\nabla_w u_h)\cdot\nabla_w v dT \\ &= \int_e \left(\mathbb{Q}_h(a\nabla_w u_h)|_{T_1}\cdot\mathbf{n}_1 + \mathbb{Q}_h(a\nabla_w u_h)|_{T_2}\cdot\mathbf{n}_2\right) v_b ds,\end{aligned}$$

where $\mathbf{n}_i$ is the outward normal direction of T_i on the edge e. Note that $\mathbf{n}_1 + \mathbf{n}_2 = 0$. Substituting the above equation into (4.5) yields

$$\int_e \left(-\mathbb{Q}_h(a\nabla_w u_h)|_{T_1} + h_{T_1}^{-1}(Q_b u_0 - u_b)|_{T_1}\mathbf{n}_1\right)\cdot\mathbf{n}_1 v_b ds = -\int_e \left(-\mathbb{Q}_h(a\nabla_w u_h)|_{T_2} + h_{T_2}^{-1}(Q_b u_0 - u_b)|_{T_2}\mathbf{n}_2\right)\cdot\mathbf{n}_2 v_b ds,$$

which shows the continuity of the numerical flux q_h in the normal direction.

5. Some technical estimates

This section shall present some technical results useful for the forthcoming error analysis. The first one is a trace inequality established in [2] for functions on general shape regular partitions. More precisely, let T be an element with e as an edge. For any function $\varphi\in H^1(T)$, the following trace inequality holds true (see [2] for details):

$$\|\varphi\|_e^2 \le C\left(h_T^{-1}\|\varphi\|_T^2 + h_T\|\nabla\varphi\|_T^2\right). \tag{5.1}$$

Another useful result is a commutativity property for some projection operators.

Lemma 5.1. *Let Q_h and $\mathbb{Q}_h$ be the L^2 projection operators defined in previous sections. Then, on each element $T\in\mathcal{T}_h$, we have the following commutative property*

$$\nabla_w(Q_h\phi) = \mathbb{Q}_h(\nabla\phi),\quad \forall\phi\in H^1(T). \tag{5.2}$$

Proof. Using (2.3), the integration by parts and the definitions of Q_h and $\mathbb{Q}_h$, we have that for any $\tau\in[P_{k-1}(T)]^d$

$$\begin{aligned}(\nabla_w(Q_h\phi),\tau)_T &= -(Q_0\phi,\nabla\cdot\tau)_T + \langle Q_b\phi,\tau\cdot\mathbf{n}\rangle_{\partial T} \\ &= -(\phi,\nabla\cdot\tau)_T + \langle\phi,\tau\cdot\mathbf{n}\rangle_{\partial T} \\ &= (\nabla\phi,\tau)_T \\ &= (\mathbb{Q}_h(\nabla\phi),\tau)_T,\end{aligned}$$

which implies the desired identity (5.2). □

The following lemma provides some estimates for the projection operators Q_h and $\mathbb{Q}_h$. Observe that the underlying mesh $\mathcal{T}_h$ is assumed to be sufficiently general to allow polygons or polyhedra. A proof of the lemma can be found in [2]. It should be pointed out that the proof of the lemma requires some non-trivial technical tools in analysis, which have also been established in [2].

Lemma 5.2. *Let $\mathcal{T}_h$ be a finite element partition of Ω that is shape regular. Then, for any $\phi \in H^{k+1}(\Omega)$, we have*

$$\sum_{T\in\mathcal{T}_h} \|\phi - Q_0\phi\|_T^2 + \sum_{T\in\mathcal{T}_h} h_T^2 \|\nabla(\phi - Q_0\phi)\|_T^2 \le Ch^{2(k+1)}\|\phi\|_{k+1}^2, \tag{5.3}$$

$$\sum_{T\in\mathcal{T}_h} \|\nabla\phi - \mathbb{Q}_h(\nabla\phi)\|_T^2 + \sum_{T\in\mathcal{T}_h} h_T^2 \|\nabla(\nabla\phi - \mathbb{Q}_h(\nabla\phi))\|_T^2 \le Ch^{2k}\|\phi\|_{k+1}^2. \tag{5.4}$$

Here and in what follows of this paper, C denotes a generic constant independent of the meshsize h and the functions in the estimates.

In the finite element space V_h, we introduce a discrete H^1 semi-norm as follows:

$$\|v\|_{1,h} = \left(\sum_{T\in\mathcal{T}_h} \left(\|\nabla v_0\|_T^2 + h_T^{-1}\|Q_b v_0 - v_b\|_{\partial T}\right)\right)^{\frac{1}{2}}. \tag{5.5}$$

The following lemma indicates that $\|\cdot\|_{1,h}$ is equivalent to the trip-bar norm (3.5).

Lemma 5.3. *There exist two positive constants C_1 and C_2 such that for any $v = \{v_0, v_b\} \in V_h$, we have*

$$C_1\|v\|_{1,h} \le |||v||| \le C_2\|v\|_{1,h}. \tag{5.6}$$

Proof. For any $v = \{v_0, v_b\} \in V_h$, it follows from the definition of weak gradient (2.4) and Q_b that

$$(\nabla_w v, q)_T = (\nabla v_0, q)_T + \langle v_b - Q_b v_0, q\cdot\rangle_{\partial T}, \quad \forall q \in [P_{k-1}(T)]^d. \tag{5.7}$$

By letting $q = \nabla_w v$ in (5.7) we arrive at

$$(\nabla_w v, \nabla_w v)_T = (\nabla v_0, \nabla_w v)_T + \langle v_b - Q_b v_0, \nabla_w v\cdot\rangle_{\partial T}.$$

From the trace inequality (5.1) and the inverse inequality we have

$$\begin{aligned}(\nabla_w v, \nabla_w v)_T &\le \|\nabla v_0\|_T\|\nabla_w v\|_T + \|Q_b v_0 - v_b\|_{\partial T}\|\nabla_w v\|_{\partial T}\\ &\le \|\nabla v_0\|_T\|\nabla_w v\|_T + Ch_T^{-1/2}\|Q_b v_0 - v_b\|_{\partial T}\|\nabla_w v\|_T.\end{aligned}$$

Thus,

$$\|\nabla_w v\|_T \le C\left(\|\nabla v_0\|_T^2 + h_T^{-1}\|Q_b v_0 - v_b\|_{\partial T}^2\right)^{\frac{1}{2}},$$

which verifies the upper bound of $|||v|||$. As for the lower bound, we chose $q = \nabla v_0$ in (5.7) to obtain

$$(\nabla_w v, \nabla v_0)_T = (\nabla v_0, \nabla v_0)_T + \langle v_b - Q_b v_0, \nabla v_0\cdot\rangle_{\partial T}.$$

Using the trace and the inverse inequality, we have

$$\|\nabla v_0\|_T^2 \le \|\nabla_w v\|_T\|\nabla v_0\|_T + Ch_T^{-1/2}\|Q_b v_0 - v_b\|_{\partial T}\|\nabla v_0\|_T.$$

This leads to

$$\|\nabla v_0\|_T \le C\left(\|\nabla_w v\|_T^2 + Ch_T^{-1}\|Q_b v_0 - v_b\|_{\partial T}^2\right)^{\frac{1}{2}},$$

which verifies the lower bound for $|||v|||$. Collectively, they complete the proof of the lemma. □

Lemma 5.4. *Assume that $\mathcal{T}_h$ is shape regular. Then for any $w \in H^{k+1}(\Omega)$ and $v = \{v_0, v_b\} \in V_h$, we have*

$$|s(Q_h w, v)| \le Ch^k\|w\|_{k+1}|||v|||, \tag{5.8}$$

$$|\ell_w(v)| \le Ch^k\|w\|_{k+1}|||v|||, \tag{5.9}$$

where $\ell_w(v) = \sum_{T\in\mathcal{T}_h}\langle a(\nabla w - \mathbb{Q}_h\nabla w)\cdot\mathbf{n},\ v_0 - v_b\rangle_{\partial T}$.

Proof. Using the definition of Q_b, (5.1), and (5.3), we obtain

$$\begin{aligned}
|s(Q_h w, v)| &= \left| \sum_{T\in\mathcal{T}_h} h_T^{-1} \langle Q_b(Q_0 w) - Q_b w,\ Q_b v_0 - v_b\rangle_{\partial T} \right| \\
&= \left| \sum_{T\in\mathcal{T}_h} h_T^{-1} \langle Q_0 w - w,\ Q_b v_0 - v_b\rangle_{\partial T} \right| \\
&\le C \left(\sum_{T\in\mathcal{T}_h} (h_T^{-2}\|Q_0 w - w\|_T^2 + \|\nabla(Q_0 w - w)\|_T^2) \right)^{\frac{1}{2}} \cdot \left(\sum_{T\in\mathcal{T}_h} h_T^{-1}\|Q_b v_0 - v_b\|_{\partial T}^2 \right)^{\frac{1}{2}} \\
&\le Ch^k \|w\|_{k+1} |||v|||.
\end{aligned}$$

As to (5.9), it follows from the Cauchy–Schwarz inequality, the trace inequality (5.1), (1.3) and the estimate (5.4) that

$$\begin{aligned}
|\ell_w(v)| &= \left| \sum_{T\in\mathcal{T}_h} \langle a(\nabla w - \mathbb{Q}_h \nabla w)\cdot \mathbf{n},\ v_0 - v_b\rangle_{\partial T} \right| \\
&\le C \sum_{T\in\mathcal{T}_h} \|a(\nabla w - \mathbb{Q}_h \nabla w)\|_{\partial T} \|v_0 - v_b\|_{\partial T} \\
&\le C \left(\sum_{T\in\mathcal{T}_h} h_T \|a(\nabla w - \mathbb{Q}_h \nabla w)\|_{\partial T}^2 \right)^{\frac{1}{2}} \left(\sum_{T\in\mathcal{T}_h} h_T^{-1} \|v_0 - v_b\|_{\partial T}^2 \right)^{\frac{1}{2}} \\
&\le Ch^k \|w\|_{k+1} \left(\sum_{T\in\mathcal{T}_h} h_T^{-1} \|v_0 - v_b\|_{\partial T}^2 \right)^{\frac{1}{2}}. \qquad (5.10)
\end{aligned}$$

Using the trace inequality (5.1) and the approximation property of the L^2 projection operator we obtain

$$\begin{aligned}
\|v_0 - v_b\|_{\partial T} &\le \|v_0 - Q_b v_0\|_{\partial T} + \|Q_b v_0 - v_b\|_{\partial T} \\
&\le Ch_T^{1/2} \|\nabla v_0\|_T + \|Q_b v_0 - v_b\|_{\partial T}.
\end{aligned}$$

Substituting the above inequality into (5.10) yields

$$|\ell_w(v)| \le Ch^k \|w\|_{k+1} \left(\sum_{T\in\mathcal{T}_h} \left\{ \|\nabla v_0\|_T^2 + h_T^{-1} \|Q_b v_0 - v_b\|_{\partial T}^2 \right\} \right)^{\frac{1}{2}}, \qquad (5.11)$$

which, along with the estimate (5.6), verifies the desired estimate (5.9). □

6. Error analysis

The goal of this section is to establish some error estimates for the weak Galerkin finite element solution u_h arising from (3.4). The error will be measured in two natural norms: the triple-bar norm as defined in (3.5) and the standard L^2 norm. The triple-bar norm is essentially a discrete H^1 norm for the underlying weak function.

For simplicity of analysis, we assume that the coefficient tensor a in (1.1) is a piecewise constant matrix with respect to the finite element partition $\mathcal{T}_h$. The result can be extended to variable tensors without any difficulty, provided that the tensor a is piecewise sufficiently smooth.

6.1. Error equation

Let $u_h = \{u_0, u_b\} \in V_h$ be the weak Galerkin finite element solution arising from the numerical scheme (3.4). Assume that the exact solution of (1.1)–(1.2) is given by u. The L^2 projection of u in the finite element space V_h is given by

$$Q_h u = \{Q_0 u, Q_b u\}.$$

Let

$$e_h = \{e_0, e_b\} = \{Q_0 u - u_0, Q_b u - u_b\}$$

be the error between the WG finite element solution and the L^2 projection of the exact solution.

Lemma 6.1. *Let e_h be the error of the weak Galerkin finite element solution arising from (3.4). Then, for any $v \in V_h^0$ we have*

$$a_s(e_h, v) = \ell_u(v) + s(Q_h u, v), \tag{6.1}$$

where $\ell_u(v) = \sum_{T\in\mathcal{T}_h} \langle a(\nabla u - \mathbb{Q}_h \nabla u)\cdot \mathbf{n}, v_0 - v_b\rangle_{\partial T}$.

Proof. Testing (1.1) by using v_0 of $v = \{v_0, v_b\} \in V_h^0$ we arrive at

$$\sum_{T\in\mathcal{T}_h} (a\nabla u, \nabla v_0)_T - \sum_{T\in\mathcal{T}_h} \langle a\nabla u\cdot \mathbf{n}, v_0 - v_b\rangle_{\partial T} = (f, v_0), \tag{6.2}$$

where we have used the fact that $\sum_{T\in\mathcal{T}_h} \langle a\nabla u\cdot \mathbf{n}, v_b\rangle_{\partial T} = 0$. To deal with the term $\sum_{T\in\mathcal{T}_h} (a\nabla u, \nabla v_0)_T$ in (6.2), we need the following equation. For any $\phi \in H^1(T)$ and $v \in V_h$, it follows from (5.2), the definition of the discrete weak gradient (2.3), and the integration by parts that

$$\begin{aligned}
(a\nabla_w Q_h\phi, \nabla_w v)_T &= (a\mathbb{Q}_h(\nabla\phi), \nabla_w v)_T \\
&= -(v_0, \nabla\cdot(a\mathbb{Q}_h\nabla\phi))_T + \langle v_b, (a\mathbb{Q}_h\nabla\phi)\cdot\mathbf{n}\rangle_{\partial T} \\
&= (\nabla v_0, a\mathbb{Q}_h\nabla\phi)_T - \langle v_0 - v_b, (a\mathbb{Q}_h\nabla\phi)\cdot\mathbf{n}\rangle_{\partial T} \\
&= (a\nabla\phi, \nabla v_0)_T - \langle (a\mathbb{Q}_h\nabla\phi)\cdot\mathbf{n},\ v_0 - v_b\rangle_{\partial T}.
\end{aligned} \tag{6.3}$$

By letting $\phi = u$ in (6.3), we have from combining (6.3) and (6.2) that

$$\begin{aligned}
\sum_{T\in\mathcal{T}_h} (a\nabla_w Q_h u, \nabla_w v)_T &= (f, v_0) + \sum_{T\in\mathcal{T}_h} \langle a(\nabla u - \mathbb{Q}_h\nabla u)\cdot\mathbf{n}, v_0 - v_b\rangle_{\partial T} \\
&= (f, v_0) + \ell_u(v).
\end{aligned}$$

Adding $s(Q_h u, v)$ to both sides of the above equation gives

$$a_s(Q_h u, v) = (f, v_0) + \ell_u(v) + s(Q_h u, v). \tag{6.4}$$

Subtracting (3.4) from (6.4) yields the following error equation,

$$a_s(e_h, v) = \ell_u(v) + s(Q_h u, v), \quad \forall v \in V_h^0.$$

This completes the proof of the lemma. □

6.2. Error estimates

The error equation (6.1) can be used to derive the following error estimate for the WG finite element solution.

Theorem 6.2. *Let $u_h \in V_h$ be the weak Galerkin finite element solution of the problem (1.1)–(1.2) arising from (3.4). Assume the exact solution $u \in H^{k+1}(\Omega)$. Then, there exists a constant C such that*

$$|||u_h - Q_h u||| \le Ch^k \|u\|_{k+1}. \tag{6.5}$$

Proof. By letting $v = e_h$ in (6.1), we have

$$|||e_h|||^2 = \ell_u(e_h) + s(Q_h u,\ e_h). \tag{6.6}$$

It then follows from (5.8) and (5.9) that

$$|||e_h|||^2 \le Ch^k \|u\|_{k+1} |||e_h|||,$$

which implies (6.5). This completes the proof. □

Next, we will measure the difference between u and u_h in the discrete H^1 semi-norm $\|\cdot\|_{1,h}$ as defined in (5.5). Note that (5.5) can be easily extended to functions in $H^1(\Omega) + V_h$ through the inclusion map i_W.

Corollary 6.3. *Let $u_h \in V_h$ be the weak Galerkin finite element solution of the problem (1.1)–(1.2) arising from (3.4). Assume the exact solution $u \in H^{k+1}(\Omega)$. Then, there exists a constant C such that*

$$\|u - u_h\|_{1,h} \le Ch^k \|u\|_{k+1}. \tag{6.7}$$

Proof. It follows from (5.6) and (6.5) that

$$\|Q_h u - u_h\|_{1,h} \le C|||Q_h u - u_h||| \le Ch^k \|u\|_{k+1}.$$

Using the triangle inequality, (5.3) and the equation above, we have

$$\|u-u_h\|_{1,h} \le \|u-Q_hu\|_{1,h} + \|Q_hu-u_h\|_{1,h} \le Ch^k\|u\|_{k+1}.$$

This completes the proof. □

In the rest of the section, we shall derive an optimal order error estimate for the weak Galerkin finite element scheme (3.4) in the usual L^2 norm by using a duality argument as was commonly employed in the standard Galerkin finite element methods [7,8]. To this end, we consider a dual problem that seeks $\Phi \in H_0^1(\Omega)$ satisfying

$$-\nabla\cdot(a\nabla\Phi) = e_0 \quad \text{in } \Omega. \tag{6.8}$$

Assume that the above dual problem has the usual H^2-regularity. This means that there exists a constant C such that

$$\|\Phi\|_2 \le C\|e_0\|. \tag{6.9}$$

Theorem 6.4. *Let $u_h \in V_h$ be the weak Galerkin finite element solution of the problem (1.1)–(1.2) arising from (3.4). Assume the exact solution $u \in H^{k+1}(\Omega)$. In addition, assume that the dual problem (6.8) has the usual H^2-regularity. Then, there exists a constant C such that*

$$\|u-u_0\| \le Ch^{k+1}\|u\|_{k+1}. \tag{6.10}$$

Proof. By testing (6.8) with e_0 we obtain

$$\begin{aligned}\|e_0\|^2 &= -(\nabla\cdot(a\nabla\Phi), e_0)\\ &= \sum_{T\in\mathcal{T}_h}(a\nabla\Phi,\ \nabla e_0)_T - \sum_{T\in\mathcal{T}_h}\langle a\nabla\Phi\cdot\mathbf{n},\ e_0-e_b\rangle_{\partial T},\end{aligned} \tag{6.11}$$

where we have used the fact that $e_b = 0$ on $\partial\Omega$. Setting $\phi = \Phi$ and $v = e_h$ in (6.3) yields

$$(a\nabla_w Q_h\Phi,\ \nabla_w e_h)_T = (a\nabla\Phi,\ \nabla e_0)_T - \langle (a\mathbb{Q}_h\nabla\Phi)\cdot\mathbf{n},\ e_0-e_b\rangle_{\partial T}. \tag{6.12}$$

Substituting (6.12) into (6.11) gives

$$\begin{aligned}\|e_0\|^2 &= (a\nabla_w e_h,\ \nabla_w Q_h\Phi) + \sum_{T\in\mathcal{T}_h}\langle a(\mathbb{Q}_h\nabla\Phi-\nabla\Phi)\cdot\mathbf{n},\ e_0-e_b\rangle_{\partial T}\\ &= (a\nabla_w e_h,\ \nabla_w Q_h\Phi) + \ell_\Phi(e_h).\end{aligned} \tag{6.13}$$

It follows from the error equation (6.1) that

$$(a\nabla_w e_h,\ \nabla_w Q_h\Phi) = \ell_u(Q_h\Phi) + s(Q_hu,\ Q_h\Phi) - s(e_h,\ Q_h\Phi). \tag{6.14}$$

By combining (6.13) with (6.14) we arrive at

$$\|e_0\|^2 = \ell_u(Q_h\Phi) + s(Q_hu,\ Q_h\Phi) - s(e_h,\ Q_h\Phi) + \ell_\Phi(e_h). \tag{6.15}$$

Let us bound the terms on the right hand side of (6.15) one by one. Using the triangle inequality, we obtain

$$\begin{aligned}|\ell_u(Q_h\Phi)| &= \left|\sum_{T\in\mathcal{T}_h}\langle a(\nabla u-\mathbb{Q}_h\nabla u)\cdot\mathbf{n},\ Q_0\Phi-Q_b\Phi\rangle_{\partial T}\right|\\ &\le \left|\sum_{T\in\mathcal{T}_h}\langle a(\nabla u-\mathbb{Q}_h\nabla u)\cdot\mathbf{n},\ Q_0\Phi-\Phi\rangle_{\partial T}\right| + \left|\sum_{T\in\mathcal{T}_h}\langle a(\nabla u-\mathbb{Q}_h\nabla u)\cdot\mathbf{n},\ \Phi-Q_b\Phi\rangle_{\partial T}\right|.\end{aligned} \tag{6.16}$$

We first use the definition of Q_b and the fact that $\Phi = 0$ on $\partial\Omega$ to obtain

$$\sum_{T\in\mathcal{T}_h}\langle a(\nabla u-\mathbb{Q}_h\nabla u)\cdot\mathbf{n}, \Phi-Q_b\Phi\rangle_{\partial T} = \sum_{T\in\mathcal{T}_h}\langle a\nabla u\cdot\mathbf{n}, \Phi-Q_b\Phi\rangle_{\partial T} = 0. \tag{6.17}$$

From the trace inequality (5.1) and the estimate (5.3) we have

$$\left(\sum_{T\in\mathcal{T}_h}\|Q_0\Phi-\Phi\|_{\partial T}^2\right)^{1/2} \le Ch^{\frac{3}{2}}\|\Phi\|_2$$

and

$$\left(\sum_{T\in\mathcal{T}_h}\|a(\nabla u-\mathbb{Q}_h\nabla u)\|_{\partial T}^2\right)^{1/2} \le Ch^{k-\frac{1}{2}}\|u\|_{k+1}.$$

Thus, it follows from the Cauchy–Schwarz inequality and the above two estimates that

$$\left|\sum_{T\in\mathcal{T}_h}\langle a(\nabla u-\mathbb{Q}_h\nabla u)\cdot\mathbf{n},\ Q_0\Phi-\Phi\rangle_{\partial T}\right| \le C\left(\sum_{T\in\mathcal{T}_h}\|a(\nabla u-\mathbb{Q}_h\nabla u)\|_{\partial T}^2\right)^{1/2}\left(\sum_{T\in\mathcal{T}_h}\|Q_0\Phi-\Phi\|_{\partial T}^2\right)^{1/2}$$
$$\le Ch^{k+1}\|u\|_{k+1}\|\Phi\|_2. \tag{6.18}$$

Combining (6.16) with (6.17) and (6.18) yields

$$|\ell_u(Q_h\Phi)| \le Ch^{k+1}\|u\|_{k+1}\|\Phi\|_2. \tag{6.19}$$

Analogously, it follows from the definition of Q_b, the trace inequality (5.1), and the estimate (5.3) that

$$\begin{aligned}|s(Q_hu,\ Q_h\Phi)| &\le \sum_{T\in\mathcal{T}_h}h_T^{-1}\,|\langle Q_b(Q_0u)-Q_bu,\ Q_b(Q_0\Phi)-Q_b\Phi\rangle_{\partial T}|\\ &\le \sum_{T\in\mathcal{T}_h}h_T^{-1}\|Q_b(Q_0u-u)\|_{\partial T}\|Q_b(Q_0\Phi-\Phi)\|_{\partial T}\\ &\le \sum_{T\in\mathcal{T}_h}h_T^{-1}\|Q_0u-u\|_{\partial T}\|Q_0\Phi-\Phi\|_{\partial T}\\ &\le C\left(\sum_{T\in\mathcal{T}_h}h_T^{-1}\|Q_0u-u\|_{\partial T}^2\right)^{1/2}\left(\sum_{T\in\mathcal{T}_h}h_T^{-1}\|Q_0\Phi-\Phi\|_{\partial T}^2\right)^{1/2}\\ &\le Ch^{k+1}\|u\|_{k+1}\|\Phi\|_2. \end{aligned}\tag{6.20}$$

The estimates (5.8) with $k=1$ and the error estimate (6.5) imply

$$|s(e_h,\ Q_h\Phi)| \le Ch\|\Phi\|_2|||e_h||| \le Ch^{k+1}\|u\|_{k+1}\|\Phi\|_2. \tag{6.21}$$

Similarly, it follows from (5.9) and (6.5) that

$$|\ell_\Phi(e_h)| \le Ch^{k+1}\|u\|_{k+1}\|\Phi\|_2. \tag{6.22}$$

Now substituting (6.19)–(6.22) into (6.15) yields

$$\|e_0\|^2 \le Ch^{k+1}\|u\|_{k+1}\|\Phi\|_2,$$

which, combined with the regularity assumption (6.9) and the triangle inequality, gives the desired optimal order error estimate (6.10). □

7. Numerical examples

In this section, we examine the WG method by testing its convergence and flexibility for solving second order elliptic problems. In the test of convergence, the first ($k=1$) and the second ($k=2$) order of weak Galerkin elements are used in the construction of the finite element space V_h. In the test of flexibility of the WG method, elliptic problems are solved on finite element partitions with various configurations, including triangular mesh, deformed rectangular mesh, and honeycomb mesh in two dimensions and deformed cubic mesh in three dimensions. Our numerical results confirm the theory developed in previous sections; namely, optimal rate of convergence in H^1 and L^2 norms. In addition, it shows a great flexibility of the WG method with respect to the shape of finite element partitions.

Let $u_h=\{u_0,u_b\}$ and u be the solution to the weak Galerkin equation and the original equation, respectively. The error is defined by $e_h=u_h-Q_hu=\{e_0,e_b\}$, where $e_0=u_0-Q_0u$ and $e_b=u_b-Q_bu$. Here $Q_hu=\{Q_0u,Q_bu\}$ with Q_h as the L^2 projection onto appropriately defined spaces. The triple-bar norm and the L^2 norm are used to measure the error in all of the numerical experiments.

7.1. Example 1

(Triangular mesh) Consider the model problem (1.1)–(1.2) in the square domain $\Omega=(0,1)\times(0,1)$. The boundary condition $u|_{\partial\Omega}=g$ and f are chosen such that the exact solution is given by $u=\sin(\pi x)\cos(\pi y)$ and

$$a=\begin{pmatrix}x^2+y^2+1 & xy\\ xy & x^2+y^2+1\end{pmatrix}.$$

The triangular mesh $\mathcal{T}_h$ used in this example is constructed by: (1) uniformly partitioning the domain into $n\times n$ sub-rectangles; (2) dividing each rectangular element by the diagonal line with a negative slope. The mesh size is denoted by

Table 7.1
Example 1. Convergence rate of lowest order WG ($k = 1$) on triangular meshes.

h	$\|\|e_h\|\|$	Order	$\|e_0\|$	Order
1/4	1.3240e+00		1.5784e+00	
1/8	6.6333e−01	9.9710e−01	3.6890e−01	2.0972
1/16	3.3182e−01	9.9933e−01	9.0622e−02	2.0253
1/32	1.6593e−01	9.9983e−01	2.2556e−02	2.0064
1/64	8.2966e−02	9.9998e−01	5.6326e−03	2.0016
1/128	4.1483e−02	1.0000	1.4078e−03	2.0004

Table 7.2
Example 2. Convergence rate of lowest order WG ($k = 1$) on triangular meshes.

h	$\|\|e_h\|\|$	$\|e_h\|$	$\|e_h\|_{\varepsilon_h}$
1/2	2.7935e−01	6.1268e−01	5.7099e−02
1/4	1.4354e−01	1.5876e−01	1.3892e−02
1/8	7.2436e−02	4.0043e−02	3.5430e−03
1/16	3.6315e−02	1.0033e−02	8.9325e−04
1/32	1.8170e−02	2.5095e−03	2.2384e−04
1/64	9.0865e−03	6.2747e−04	5.5994e−05
1/128	4.5435e−03	1.5687e−04	1.4001e−05
1/256	2.2718e−03	3.9219e−05	3.5003e−06
$O(h^r)$, $r =$	9.9388e−01	1.9931	1.9961

Table 7.3
Example 2. Convergence rate of second order WG ($k = 2$) on triangular meshes.

h	$\|\|e_h\|\|$	$\|e_h\|$	$\|e_h\|_{\varepsilon_h}$
1/2	1.7886e−01	9.4815e−02	3.3742e−02
1/4	4.8010e−02	1.2186e−02	4.9969e−03
1/8	1.2327e−02	1.5271e−03	6.6539e−04
1/16	3.1139e−03	1.9077e−04	8.5226e−05
1/32	7.8188e−04	2.3829e−05	1.0763e−05
1/64	1.9586e−04	2.9774e−06	1.3516e−06
1/128	4.9009e−05	3.7210e−07	1.6932e−07
1/256	1.2260e−05	4.6500e−08	2.1160e−08
$O(h^r)$, $r =$	1.9813	2.9967	2.9559

$h = 1/n$. The lowest order ($k = 1$) weak Galerkin element is used for obtaining the weak Galerkin solution $u_h = \{u_0, u_b\}$; i.e., u_0 and u_b are polynomials of degree $k = 1$ and degree $k - 1 = 0$ respectively on each element $T \in \mathcal{T}_h$.

Table 7.1 shows the convergence rate for WG solutions measured in H^1 and L^2 norms. The numerical results indicate that the WG solution of linear element is convergent with rate $O(h)$ in H^1 and $O(h^2)$ in L^2 norms.

7.2. Example 2

(Triangular mesh) In the second example, we consider the Poisson problem that seeks an unknown function $u = u(x, y)$ satisfying

$$-\Delta u = f$$

in the square domain $\Omega = (0, 1)^2$. Like the first example, the exact solution here is given by $u = \sin(\pi x)\cos(\pi y)$ and g and f are chosen accordingly to match the exact solution.

The very same triangular mesh is employed in the numerical calculation. Associated with this triangular mesh $\mathcal{T}_h$, two weak Galerkin elements with $k = 1$ and $k = 2$ are used in the computation of the weak Galerkin finite element solution u_h. For simplicity, these two elements shall be referred to as $(P_1(T), P_0(e))$ and $(P_2(T), P_1(e))$.

Tables 7.2 and 7.3 show the numerical results on rate of convergence for the WG solutions in H^1 and L^2 norms associated with $k = 1$ and $k = 2$, respectively. Note that $\|e_h\|_{\varepsilon_h}$ is a discrete L^2 norm for the approximation u_b on the boundary of each element. Optimal rates of convergence are observed numerically for each case.

7.3. Example 3

(Quadrilateral mesh) In this test, we solve the same Poisson equation considered in the second example by using quadrilateral meshes.

We start with an initial quadrilateral mesh, shown as in Fig. 7.1 (Left). The mesh is then successively refined by connecting the barycenter of each coarse element with the middle points of its edges, shown as in Fig. 7.1 (Right). For this deformed

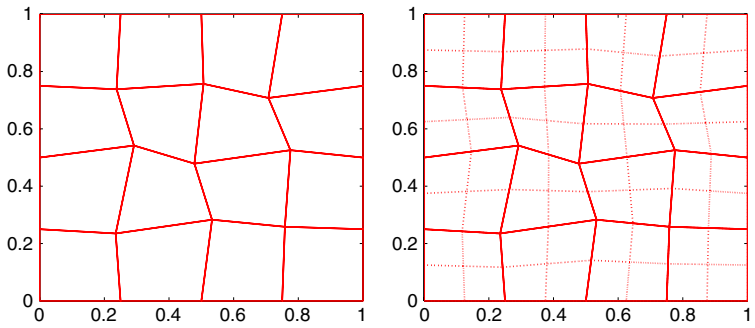

Fig. 7.1. Mesh level 1 (Left) and mesh level 2 (Right) for example 3.

Table 7.4
Example 3. Error and rate of convergence for first order WG ($k = 1$) on quadrilateral meshes.

h	$\|\|e_h\|\|$	Order	$\|e_0\|$	Order
2.9350e−01	1.9612e+00		2.1072e+00	
1.4675e−01	1.0349e+00	9.2225e−01	5.7219e−01	1.8808
7.3376e−02	5.2434e−01	9.8094e−01	1.4458e−01	1.9847
3.6688e−02	2.6323e−01	9.9418e−01	3.5655e−02	2.0197
1.8344e−02	1.3179e−01	9.9808e−01	8.6047e−03	2.0509
9.1720e−03	6.5925e−02	9.9934e−01	2.0184e−03	2.0919

Table 7.5
Example 4. Error and rate of convergence for second order WG ($k = 2$) on rectangular meshes.

h	$\|\|e_h\|\|$	Order	$\|e_0\|$	Order
1/2	1.7955e−01		1.4891e−01	
1/4	8.7059e−02	1.0444	1.8597e−02	3.0013
1/8	2.8202e−02	1.6262	2.1311e−03	3.1254
1/16	7.8114e−03	1.8521	2.4865e−04	3.0995
1/32	2.0347e−03	1.9408	2.9964e−05	3.0528
1/64	5.1767e−04	1.9747	3.6806e−06	3.0252
1/128	1.3045e−04	1.9885	4.5627e−07	3.0120

quadrilateral mesh $\mathcal{T}_h$, Table 7.4 shows the rate of convergence for the WG solutions in H^1 and L^2 norms associated with $k = 1$. It is noted that the rate of convergence is optimal for errors measured in H^1-norm and L^2-norm.

7.4. Example 4

(Rectangular mesh) The same setting of Poisson equation as Example 2 is tested again on uniform rectangular mesh for higher order weak Galerkin element.

WG element with $k = 2$ is chosen for testing. Table 7.5 shows that the numerical error of WG approximation measured in H^1-norm converges with rate $O(h^2)$ and the error measured in L^2-norm converges with rate $O(h^3)$, which agrees very well with our theoretical results.

7.5. Example 5

(Honeycomb mesh) In the fifth test, we solve the Poisson equation on the domain of unit square with exact solution $u = \sin(\pi x)\sin(\pi y)$. The Dirichlet boundary data g and f are chosen to match the exact solution. The numerical experiment is performed on the honeycomb mesh as shown in Fig. 7.2. The linear WG element ($k = 1$) is used in this numerical computation.

The error profile is presented in Table 7.6, which confirms the convergence rates predicted by the theory.

7.6. Example 6

(Deformed cubic mesh) In the last numerical experiment, the Poisson equation is solved on a three dimensional domain $\Omega = (0, 1)^3$. The exact solution is chosen as

$$u = \sin(2\pi x)\sin(2\pi y)\sin(2\pi z),$$

and the Dirichlet boundary data g and f are chosen accordingly to match the exact solution.

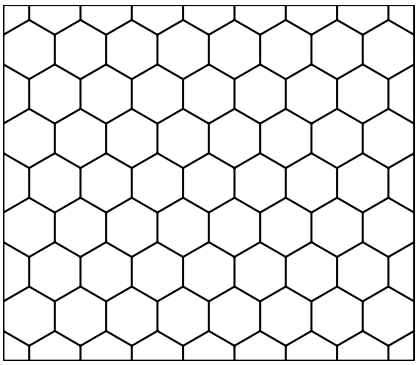

Fig. 7.2. Honeycomb mesh for example 5.

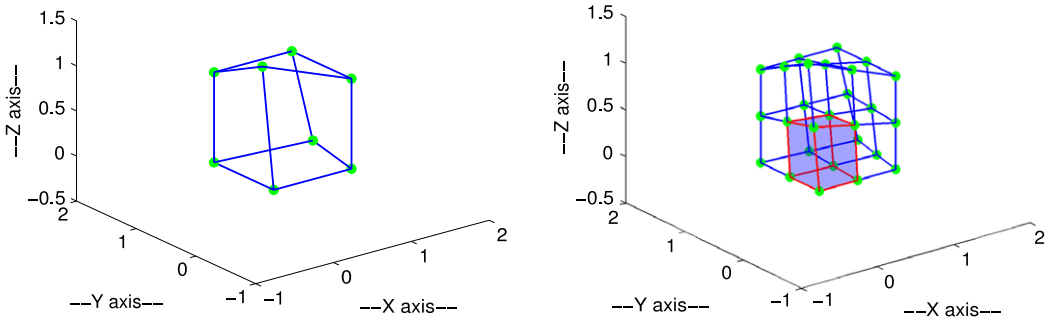

Fig. 7.3. Mesh level 1 (Left) and mesh level 2 (Right) for example 6.

Table 7.6
Example 5. Error and rate of convergence for linear WG element ($k = 1$) on honeycomb meshes.

h	$\|\|e_h\|\|$	Order	$\|e_0\|$	Order
1.6667e−01	3.3201e−01		1.6006e−02	
8.3333e−02	1.6824e−01	9.8067e−01	3.9061e−03	2.0347
4.1667e−02	8.4784e−02	9.8867e−01	9.6442e−04	2.0180
2.0833e−02	4.2570e−02	9.9392e−01	2.3960e−04	2.0090
1.0417e−02	2.1331e−02	9.9695e−01	5.9711e−05	2.0047
5.2083e−03	1.0677e−02	9.9839e−01	1.4904e−05	2.0022

Table 7.7
Example 6. Error and convergence rate for $k = 1$ on deformed cubic mesh.

h	$\|\|e_h\|\|$	Order	$\|e_0\|$	Order
1/2	5.7522		9.1990	
1/4	1.3332	2.1092	1.5684	2.5522
1/8	6.4071e−01	1.0571	2.7495e−01	2.5121
1/16	3.2398e−01	9.8377e−01	6.8687e−02	2.0011
1/32	1.6201e−01	9.9982e−01	1.7150e−02	2.0018

Deformed cubic meshes are used in this test, see Fig. 7.3 (Left) for an illustrative element. The construction of the deformed cubic mesh starts with a coarse mesh. The next level of mesh is derived by refining each deformed cube element into 8 sub-cubes, as shown in Fig. 7.3 (Right). Table 7.7 reports some numerical results for different level of meshes. It can be seen that a convergent rate of $O(h)$ in H^1 and $O(h^2)$ in L^2 norms are achieved for the corresponding WG finite element solutions. This confirms the theory developed in earlier sections.

Acknowledgments

The research of Wang was supported by the NSF IR/D program, while working at National Science Foundation. However, any opinion, finding, and conclusions or recommendations expressed in this material are those of Wang and do not

necessarily reflect the views of the National Science Foundation. The third author's research was supported in part by National Science Foundation Grant DMS-1115097.

References

[1] J. Wang, X. Ye, A weak Galerkin finite element method for second-order elliptic problems, J. Comput. Appl. Math. 241 (2013) 103–115. arXiv:1104.2897v1.
[2] J. Wang, X. Ye, A weak Galerkin mixed finite element method for second-order elliptic problems, Math. Comp. 83 (2014) 2101–2126. arXiv:1202.3655v1.
[3] L. Mu, J. Wang, X. Ye, Weak Galerkin finite element method for second-order elliptic problems on polytopal meshes, Int. J. Numer. Anal. Model. 12 (2015) 31–53.
[4] B. Cockburn, J. Gopalakrishnan, R. Lazarov, Unified hybridization of discontinuous Galerkin, mixed, and continuous Galerkin methods for second order elliptic problems, SIAM J. Numer. Anal. 47 (2009) 1319–1365.
[5] L. Mu, J. Wang, X. Ye, Weak Galerkin finite element methods for the biharmonic equation on polytopal meshes, Numer. Methods Partial Differential Equations 30 (2014) 1003–1029. arXiv:1303.0927.
[6] C. Wang, J. Wang, An efficient numerical scheme for the biharmonic equation by weak Galerkin finite element methods on polygonal or polyhedral meshes, Comput. Math. Appl. 68 (2014) 2314–2330.
[7] P.G. Ciarlet, The Finite Element Method for Elliptic Problems, North-Holland, New York, 1978.
[8] S. Brenner, R. Scott, The Mathematical Theory of Finite Element Mathods, Springer-Verlag, New York, 1994.